EXPERIMENTAL TECHNIQUE AND DEVICES

Original article
DOI: https://doi.org/10.18721/JPM.18407

APPLICATION OF FRACTAL METHODS FOR ANALYZING THE MICRODEFORMATION DATA OF THE EARTH'S CRUST

A. S. Lisovitsky[1]✉, *V. A. Chupin*[1], *L. G. Moskovchenko*[2]

[1] V. I. Il'ichev Pacific Oceanological Institute, Vladivostok, Russia;

[2] Far Eastern Federal University, Vladivostok, Russia

✉ lisovitckii.as@poi.dvo.ru

Abstract. In the paper, the changes in microdeformations of the Earth's crust have been studied using methods of the fractal and multifractal analyses. Most attention was concentrated on revealing the regularities of the changes in the fractal dimension and singularity power exponents of the data obtained experimentally using laser strainmeters during periods preceding earthquakes. The fractal dimension was found to increase before seismic events, especially according to the data from the laser strainmeter located on a bedrock base. Our analysis exhibited a decrease in the amplitude and singularity power exponents during active periods. The results obtained confirm the considerable promise of applying the fractal methods for monitoring the microdeformations of the Earth's crust and predicting earthquakes.

Keywords: microdeformation of the Earth's crust, self-organized criticality, fractal analysis, laser strainmeter

Funding: The research was supported by state budget theme "Study of the nature of linear and nonlinear interactions of geospheric fields of transition zones of the World Ocean and their consequences" (No. 124022100074-9) of V. I. Il`ichev Pacific Oceanological Institute, Far Eastern Branch of the Russian Academy of Sciences (Vladivostok, Russia).

Citation: Lisovitsky A. S., Chupin V. A., Moskovchenko L. G., Application of fractal methods for analyzing the microdeformation data of the Earth's crust, St. Petersburg State Polytechnical University Journal. Physics and Mathematics. 18 (4) (2025) 101–113. DOI: https://doi.org/10.18721/JPM.18407

Научная статья
УДК 550.343
DOI: https://doi.org/10.18721/JPM.18407

ПРИМЕНЕНИЕ ФРАКТАЛЬНЫХ МЕТОДОВ ДЛЯ АНАЛИЗА ДАННЫХ МИКРОДЕФОРМАЦИЙ ЗЕМНОЙ КОРЫ

А. С. Лисовицкий[1]✉, *В. А. Чупин*[1], *Л. Г. Московченко*[2]

[1] Тихоокеанский океанологический институт им. В. И. Ильичёва Дальневосточного отделения РАН, г. Владивосток, Россия;

[2] Дальневосточный федеральный университет, г. Владивосток, Россия

✉ lisovitckii.as@poi.dvo.ru

Аннотация. В работе исследованы изменения микродеформаций земной коры с использованием методов фрактального и мультифрактального анализов. Основное внимание уделено выявлению закономерностей изменения фрактальной размерности

и степенных показателей сингулярности данных, полученных экспериментально, с помощью лазерных деформографов, в периоды, предшествующие землетрясениям. Установлено, что фрактальная размерность возрастает перед сейсмическими событиями, особенно согласно данным с лазерного деформографа, расположенного на скальном основании. Анализ продемонстрировал снижение амплитуды и степенных показателей сингулярности в активные периоды. Полученные результаты подтверждают перспективность применения фрактальных методов для мониторинга микродеформаций земной коры и предсказания землетрясений.

Ключевые слова: микродеформация земной коры, самоорганизованная критичность, фрактальный анализ, лазерный деформограф

Финансирование: Работа выполнена при финансовой поддержке госбюджетной темы ТОИ ДВО РАН (г. Владивосток, Россия) № 124022100074-9 «Изучение природы линейного и нелинейного взаимодействия геосферных полей переходных зон Мирового океана и их последствий».

Ссылка для цитирования: Лисовицкий А. С., Чупин В. А., Московченко Л. Г. Применение фрактальных методов для анализа данных микродеформаций земной коры // Научно-технические ведомости СПбГПУ. Физико-математические науки. 2025. Т. 18. № 4. С. 101–113. DOI: https://doi.org/10.18721/JPM.18407

Introduction

Low-frequency microseismic oscillations serve as a valuable source of data on geodynamic processes in the Earth's crust. Such wave-like motions are continuous low-amplitude oscillations of the Earth's surface, which are caused by atmospheric and oceanic processes. These include so-called silent earthquakes and slow motions of the crust's upper layers, as well as significant fluctuations in atmospheric pressure, cyclones, hurricanes, and the impact of oceanic waves on the coastline and shelf.

The Earth's crust serves as a medium through which seismic waves propagate. The characteristics of the signals propagating in the Earth's crust vary depending on its state. Statistical parameters of the microseismic field may reflect changes in the crust's properties, including processes preceding strong earthquakes.

One of the most promising approaches to analysis of such systems is offered by fractal methods, which make it possible to study the structure of time series, assess their complexity, and identify hidden patterns that may precede catastrophic events. Fractal characteristics, such as fractal dimension and multifractal spectra, reflect changes in the dynamics of the system and are sensitive to perturbations of its equilibrium.

This paper applies fractal and multifractal analysis methods for processing laser strainmeter readings to study microdeformations of the Earth's crust.

The main focus is on identifying patterns in the dynamics of fractal characteristics, developing criteria for their predictive capability, and evaluating their applicability to earthquake prediction.

The key point of this approach is to use data from microdeformations of the Earth's crust, unlike most previous studies based on analysis of traditional seismograms or GPS observations.

The combination of multifractal detrended fluctuation analysis (MF-DFA) and the Higuchi method for estimating the fractal dimension made it possible to comprehensively analyze the structure of time series and identify the patterns preceding earthquakes.

Self-organized criticality and fractality of the Earth's crust

The lithosphere, consisting of many blocks, is subjected to elastic stresses, absorbing additional energy from the external environment and transferring it between the blocks. When the level of accumulated elastic energy in a lithospheric block reaches a critical value, this block becomes unstable, which can lead to its displacement or fracture. This instability is characterized

by a state where small external perturbations can induce significant changes, while the system continues to evolve without reaching equilibrium, remaining in a state close to critical. The described behavior is characteristic of systems with self-organized criticality: such a system reaches a state in which large-scale processes occur at various levels, independent of external triggers. Interactions between system elements become sensitive to small changes, which leads to complex and unpredictable events.

To explain these phenomena, Bak, Tang and Wiesenfeld [1] proposed the concept of self-organized criticality. This concept describes a system that, in the course of its evolution, arrives at a self-organized critical state where its behavior is characterized by fractal structure, minimal stability, and spatial scaling at different levels [1].

For further discussion, let us define seismic periods.

A seismically active period is a time interval that includes earthquakes with magnitude 7 or higher (on the Richter scale), as well as several months of pre-seismic crustal deformation preceding the event.

A seismically quiet period is a time interval during which no earthquakes with a magnitude higher than 6 occur (taking into account the geographical region).

Fractal methods of time series analysis

One of the main methods for fractal analysis of geophysical data series uses the fractal length L. There are several implementations of the algorithm for calculating $L(n)$, where n is the number of iterations.

In particular, the Higuchi method involves, for a series

$$Y(j), \text{ where } j = 1, 2, \ldots, N,$$

performing n iterations for each $L(n)$.

The length of the curve is calculated from the points corresponding to the moments

$$m, m + n, m + 2n,$$

where $m = 1, 2, \ldots, n$ (m is the initial shift);

$$L_m(n) = \left(\sum_{i=1}^{\frac{N-m}{n}} Y(m+i\cdot n) - Y(m+(i-1)\cdot n) \right) \cdot \left[\frac{N-1}{\frac{N-m}{n}\cdot n} \right], \quad (1)$$

where $(N - 1)/\{[(N - m)/n]n\}$ is the normalizing factor; $[(N - m)/n]$ is the largest integer value not exceeding the $(N - m)/n$.

Finally, the length of the curve is defined as the arithmetic mean over n values, each of which is $L_m(n)$.

Next, the average value $\langle L(n) \rangle$ over all m is calculated and the dependence of log $\langle L(n) \rangle$ on log(n) is plotted. This dependence is then approximated by a straight line using the least squares method.

The resulting straight line is described by the equation

$$y = -D \cdot x + b, \quad (2)$$

where D is the required fractal dimension.

We obtain Eq. (2) after linear approximation of the graph [2].

Time series analysis is also performed using the MF-DFA method, which includes several stages [3].

Stage I. A fluctuation profile of the following form is calculated:

$$Y(k) = \sum_{i=1}^{k} \left(z(i) - \bar{z} \right), \quad (3)$$

where $z(i)$ is the initial time series.

Stage II. The profile $Y(k)$ should be divided into non-overlapping segments s of equal length. A similar procedure is repeated from the opposite end to account for the entire fluctuation profile.

Stage III. The local trend is calculated for each of the $2N_s$ segments using the least squares method. Then the variance $F^2(v,s)$

$$F^2(v,s) = \frac{1}{s}\sum_{i=1}^{s}\left\{Y\left[(\nu-1)\cdot s + i\right] - y_v(i)\right\}^2 \tag{4}$$

is determined for each segment v ($v = 1, 2, ..., N_s$) and

$$F^2(v,s) = \frac{1}{s}\sum_{i=1}^{s}\left\{Y\left[N - (\nu - N_s)\cdot s + i\right] - y_v(i)\right\}^2 \tag{5}$$

for $v = N_s + 1, N_s + 2, ..., 2N_s$, where $y_v(i)$ is the approximating polynomial in the segment v.

Stage IV. All segments are averaged to obtain the qth order of the fluctuation functions

$$F_q(s) = \left\{\frac{1}{s}\sum_{\nu=1}^{2N_s}\left[F^2(\nu,s)\right]^{\frac{q}{2}}\right\}^2, \tag{6}$$

where q is the moment order of the fluctuation function (which can take only real values).

The value of the generalized Hurst exponent $h(0)$ corresponds to the logarithmic average of the fluctuation function and cannot be calculated directly due to the singularity in Eq. (6). In this case, a logarithmic averaging procedure is used:

$$F_0(s) = \exp\left[\frac{1}{4N_s}\sum_{\nu=1}^{2N_s}\ln F^2(\nu,s)\right]$$

Stage V. The scaling behavior of the fluctuation functions is determined by analyzing the graphs of each of the q values plotted along the axes $F_q(s)$ and s on a logarithmic scale. The main multifractal characteristics are determined: the generalized Hurst exponent $h(q)$, reflecting the degree of long-term correlation of the signal, and the singularity power exponent $\alpha(q)$, characterizing the degree of signal singularity.

$$F_q(s) \sim s^{h(q)},\ \tau(q) = h(q)\cdot q - 1,\ \alpha(q) = d\tau(q)/dq.$$

Experimental setup

Laser strainmeters based on the Michelson interferometer were used for the study.

The operating principle is as follows. The laser beam enters the interference unit, where it is split by a semi-transparent plate into two beams: the reflected beam and the transmitted beam. Both beams reflect off flat mirrors, return to the semi-transparent plate and form an interference pattern, recorded by the detector.

The work uses single-axis laser strainmeters based on the unequal-arm principle.

We used experimental data obtained during four major earthquakes to study their fractal characteristics, which could indicate impending seismic events. These data were collected from strainmeters measuring the microdeformations of the Earth's crust throughout four seismically active periods during which one or more earthquakes occurred.

The quiet seismic period when no earthquakes with a magnitude above 6 occurred was the time interval from April 1 to June 30, 2017. The geographical location of the earthquakes and their key characteristics are given in Table (see also Fig. 1).

The Cape Schultz Marine Experimental Station (see Fig. 1) is part of the V.I. Il'ichev Pacific Oceanological Institute of the Far Eastern Branch of the Russian Academy of Sciences (Vladivostok, Russia). The station houses a hardware and software system comprising the following main structural elements.

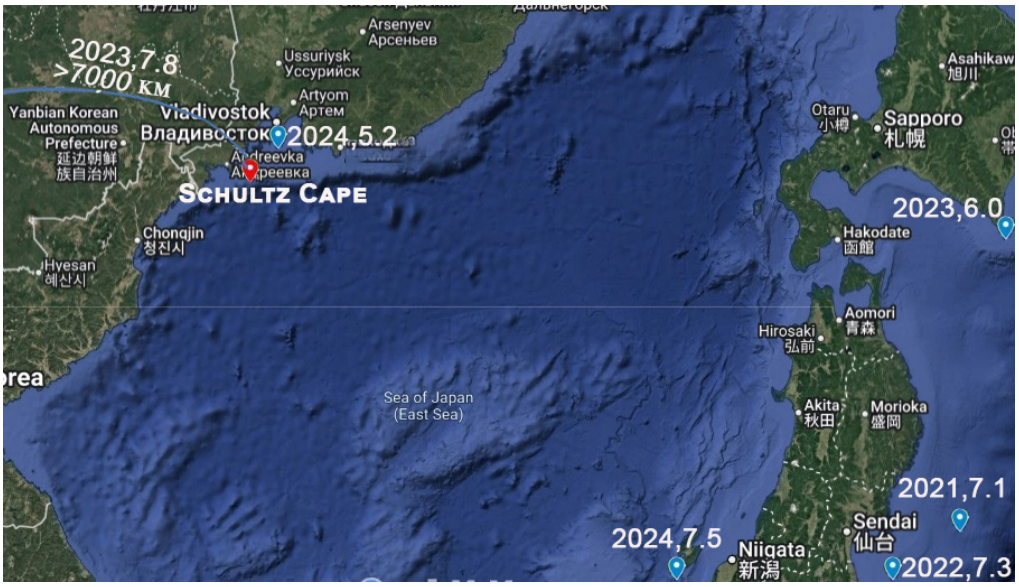

Fig. 1. Location, year of event, and magnitude of earthquakes considered
The red marker indicates the position of Cape Shultz Marine Experimental Station equipped with laser strainmeters recording data on microdeformations of the Earth's crust during earthquakes

Table

Earthquakes observed during seismically active periods

Period	Date	Location	Magnitude, points	Depth, km
01.10.2020–31.03.2021	20.03.2021	30 km from Ishinomaki (Japan)	7.0	43
	13.02.2021	34 km from Namie (Japan)	7.1	44
15.01–16.03.2022	21.01.2022	27 km from Namie (Japan)	6.3	39
	16.03.2022	57 km from Namie (Japan)	7.3	41
01.12.2022–15.02.2023	06.02.2023	Pazarcık (Turkey)	7.8	10
	16.01.2023	Hokkaido Island (Japan)	6.0	55
01.12.2023–29.02.2024	27.12.2023	Peter the Great Gulf (Russia, Primorsky Krai)	5.2	410
	01.01.2024	Noto Peninsula (Japan)	7.5	10

I. Classical laser strainmeter with unequal-arm configuration, designed to record displacement variations for a crustal section with the length equal to that of the strainmeter's measuring arm (52.5 m) in the frequency range from 10^{-3} Hz to 1 kHz with an accuracy of 0.01 nm.

II. Classical laser strainmeter with unequal-arm configuration and measuring arm length of 17.5 m.

III. Pendulum-type strainmeter with unequal-arm configuration and measuring arm length of 52.5 m.

Other hardware elements of the measuring systems are not described here, as they are secondary to this study.

Strainmeters I and III are oriented approximately north–south, at an 18° angle to the meridian, but are installed on different parallel sites: I is on sandy soil, while III is on bedrock. Strainmeter II is oriented perpendicular to I and III and is installed on heavy loam.

Experimental data (digital and analog) are transmitted to the laboratory for processing and storage, building a data bank. All systems, equipped with four computers, are connected into a single network and use a precision clock synchronizing the data with an accuracy ranging from 100 to 10 ns [4].

The obtained data were analyzed in the MatLab environment. Graphs reflecting the dynamics of fractal characteristics during the studied periods were plotted as output data. Analysis of the relationship between the required fractal dimension D and the function $\alpha(q)$ characterizing the degree of signal singularity is beyond the scope of this work, therefore it was not carried out and will be the subject of future research.

Results of fractal analysis

Analyzing the processed experimental data obtained from Strainmeters I–III, we can formulate the following conclusions.

Results for fractal variables. Firstly, the values of the fractal dimension D increase before earthquakes; this is especially pronounced in the data from Strainmeter III (Fig. 2).

Secondly, we should consider the behavior of the quantity $\Delta\alpha$, the difference between the maximum and minimum values of the singularity exponent. A decrease in the spread of this quantity and a decrease in its amplitude are observed during seismically active periods, compared to quiet periods, which makes the graphs smoother. Significant amplitude variations and high values of the quantities obtained from Strainmeters II and III were recorded in the period from December 1, 2022 to February 15, 2023 (Fig. 3).

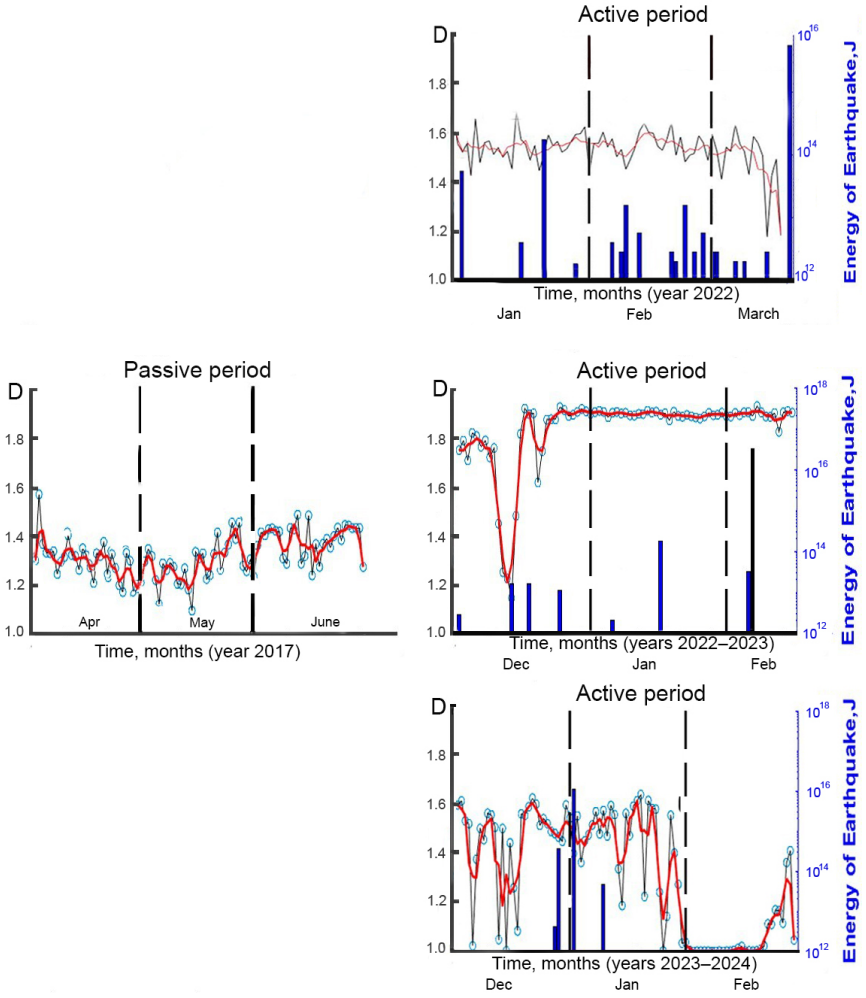

Fig. 2. Comparison of variation in fractal dimension D and earthquake energy (right axes) based on the data from Strainmeter III The plots on the left correspond to the quiet period, plots on the right correspond to the active period.
The red curves correspond to the data averaged by the sliding window method (window size: 5 measurements)

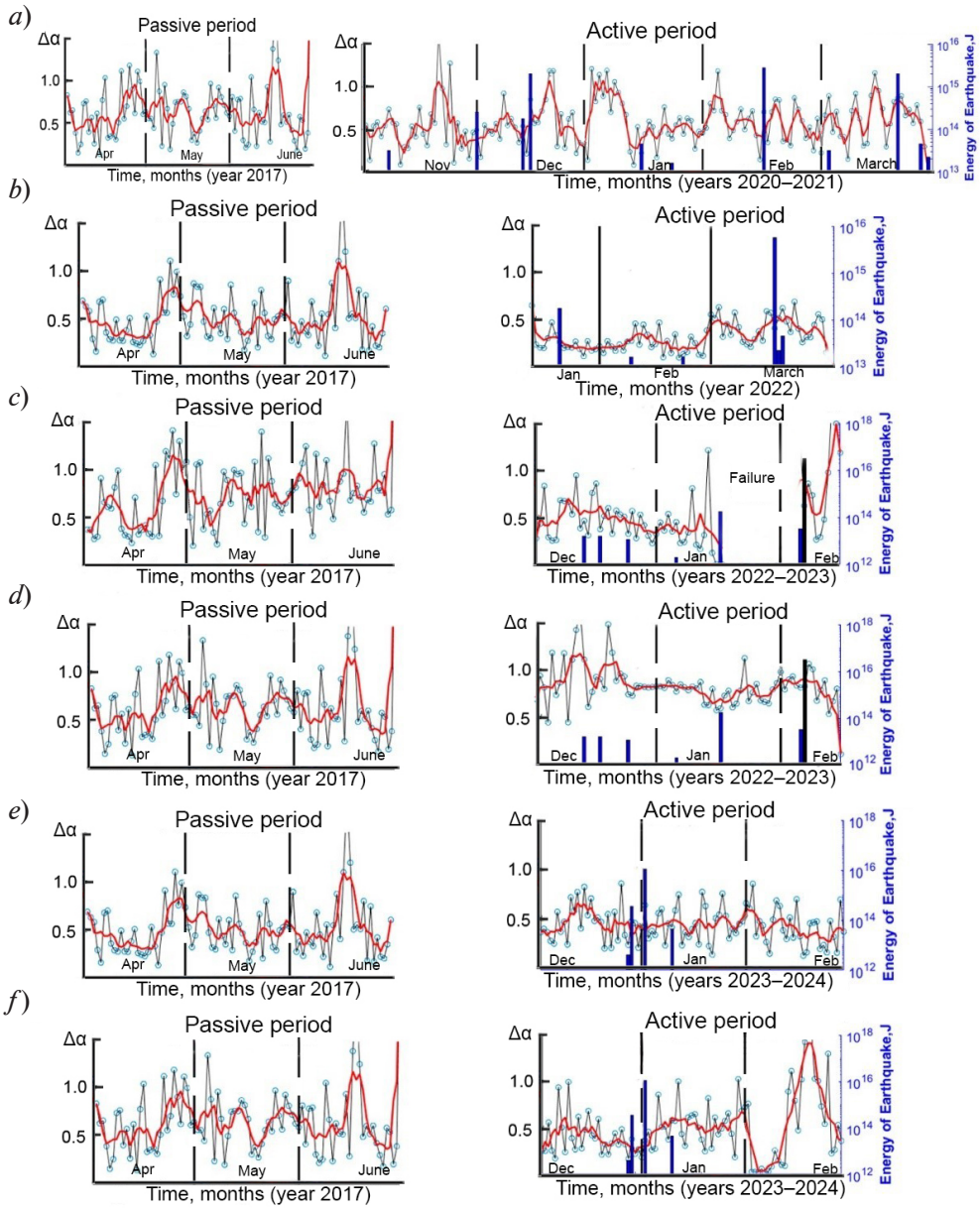

Fig. 3. Variations in width of multifractal spectrum Δα for all selected periods (see Table) \ and based on the data from Strainmeters I (*a*, *c*), II (*b*, *e*) and III (*d*, *f*)
The graphs of quiet periods are shown side by side for ease of comparison

Analyzing the relationship between the fractal dimension D and the width of the multifractal spectrum Δα based on the experimental data, we found only a weak linear correlation between these parameters (Fig. 4). Approximating the dependence $D(\Delta\alpha)$ by the least squares method, we could estimate the determination coefficient $R^2 \approx 0.30$, which indicates that the linear model accounts for only about 30% of the variance of the fractal dimension due to variations in the width of the multifractal spectrum. This observation suggests that changes in these parameters reflect different aspects of the multifractal structure of the microdeformation time series; the changes do not always occur synchronously.

Thirdly, the minimum value of the singularity exponent α_{min} shows a decrease in the periods from December 1, 2022 to February 15, 2023, and from December 1, 2023 to February 29, 2024 The α_{min} values obtained from the three strainmeters exhibit different behavior for the period from January 1 to March 16, 2022, similar to the period from October 1, 2020 to March 31, 2021, although this difference is less pronounced.

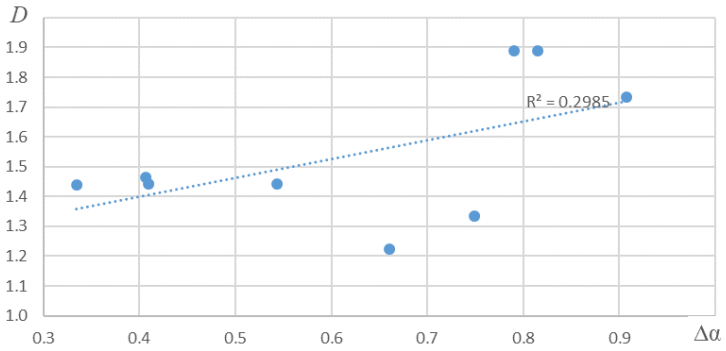

Fig. 4. Experimental (dots) and approximating (dotted line) dependences of fractal dimension D on width of multifractal spectrum $\Delta\alpha$ (R^2 is the determination coefficient)

Fourthly, each strainmeter yielded different behaviors for the maximum value of the singularity exponent α_{max}.

Results for strainmeter data Strainmeter I: slight differences are observed in the behavior of all the studied parameters during the relatively quiet period. The average values of the parameters only differ slightly. However, a greater spread in the parameter values is observed during the quiet period.

Strainmeter II: variations in the behavior of the parameters are more pronounced, especially for the fractal dimension D in the periods from December 1, 2022 to February 15, 2023 and from December 1, 2023 to February 29, 2024.

Strainmeter III: significant variations are observed, especially in the period from December 1, 2022 to February 15, 2023 (Fig. 5).

Results for selected periods. Two closely located earthquakes of significant magnitude occurred during the seismically active periods from October 1, 2020 to March 31, 2021 and from January 15 to March 16, 2022 (see Table). It is worth noting that both periods are characterized by similar values of the fractal dimension D and similar values of the multifractal spectrum width $\Delta\alpha$ (Fig. 6).

The function $\alpha(q)$ was calculated in the range of q values from -5 to +5, in increments of 0.5. This range was chosen to account for both strong and weak fluctuations and detect the characteristics of the multifractal structure of the time series.

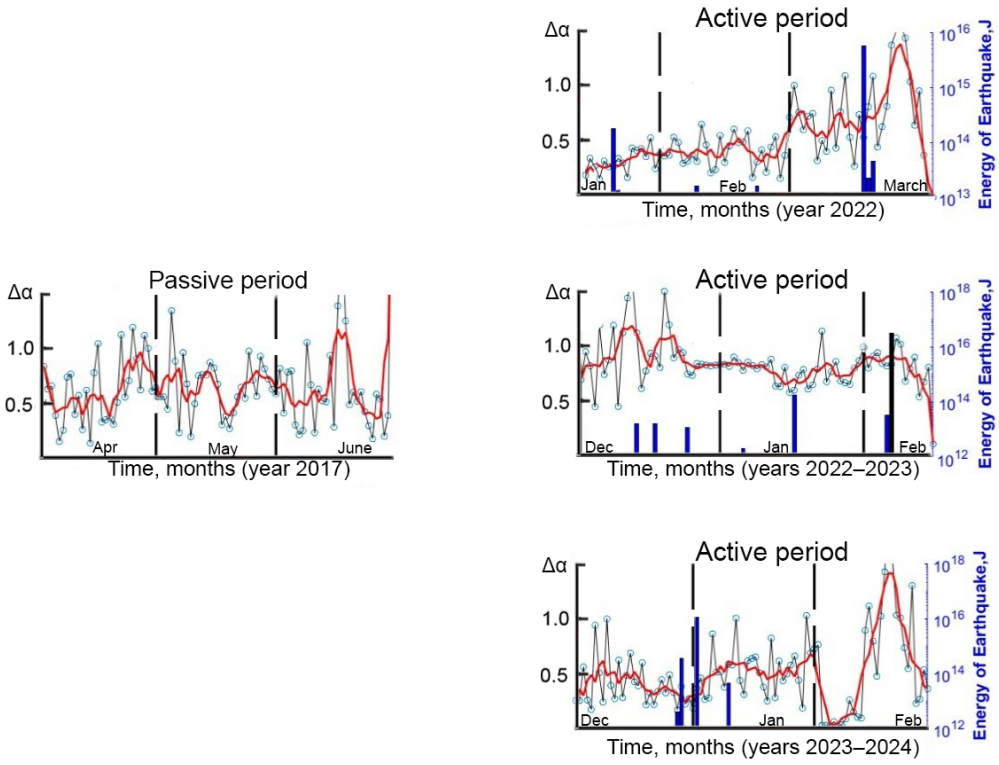

Fig. 5. Variations in width of multifractal spectrum $\Delta\alpha$ based on the data from Strainmeter III

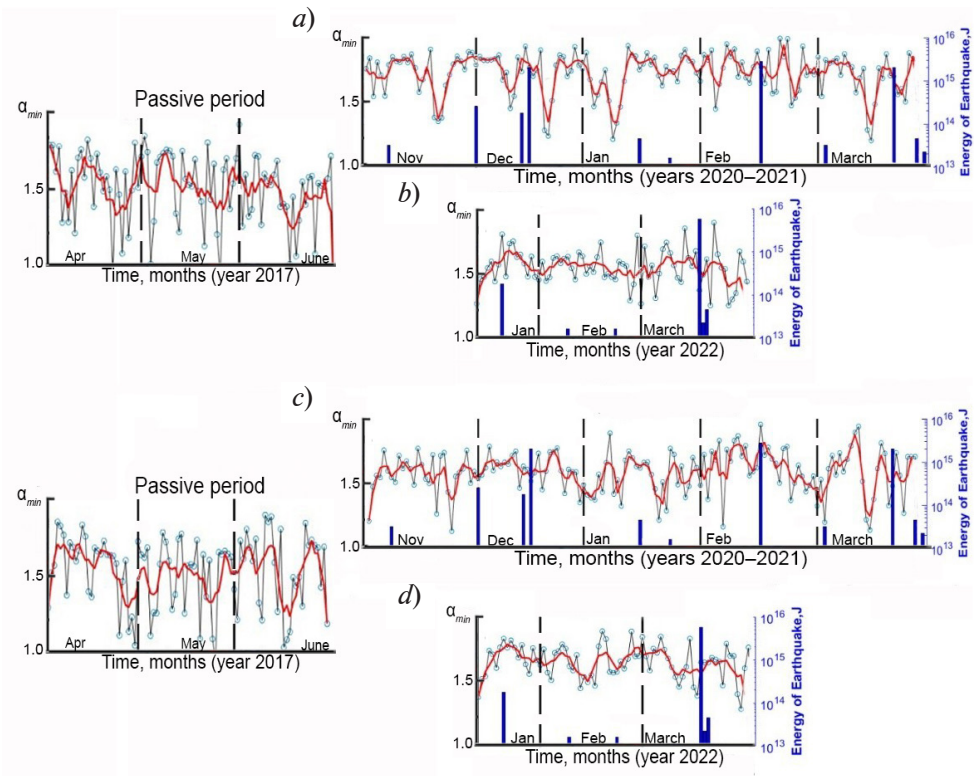

Fig. 6. Variations in α_{min} based on the data from Strainmeters I (*a*, *b*) and II (*c*, *d*) during two periods: from October 1, 2020 to March 31, 2021 and from January 15 to March 16, 2022

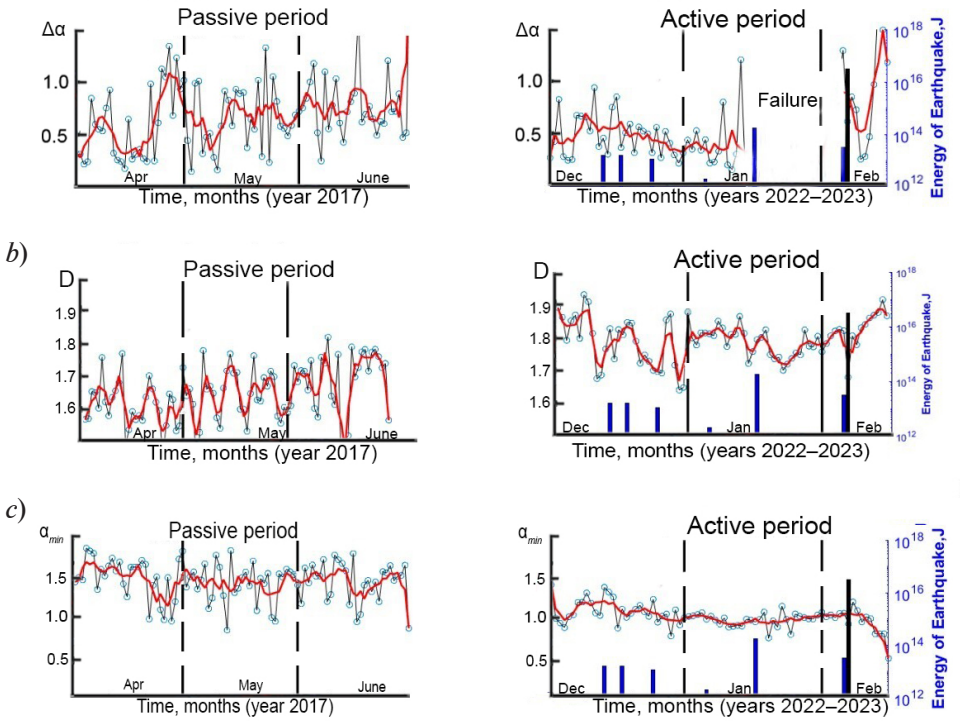

Fig. 7. Variations in parameters Δα, α_{min} and *D* from December 1, 2022 to February 15, 2023 based on the data from Strainmeters I (*a*), II (*b*) and III (*c*)

The period from December 1, 2022 to February 15, 2023 is characterized by significant variation in the values of fractal characteristics, compared with the quiet period and other active periods. This fact is difficult to explain by the earthquakes occurring in this period (see Table). It is assumed that the data from the strainmeters were influenced by other seismic events (Fig. 7).

The seismically active period from December 1, 2023 to February 29, 2024 is interesting because two earthquakes occurred in close proximity to the strainmeters. Notably, the data obtained from all strainmeters during this period exhibit the same patterns of behavior.

In conclusion, let us focus in more detail on the behavior of the fractal dimension D. In general, an increase in the fractal dimension D is observed during earthquake preparation periods. However, the accuracy with which D is determined depends on the degree of scatter of the points on the log–log plots, which was not explicitly assessed in this study.

The variations in D are more pronounced for Strainmeter III (installed on bedrock): its values lie in the range $1.0 < D < 1.7$ in active periods, and in the range $1.0 < D < 1.4$ in quiet periods. Peaks on the curves of the time series for D, reaching values up to $D \approx 1.6$ and above, may indicate nonlinear behavior and the system's impending transition to a critical state Values of D close to unity may indicate the end of the current trend, although this interpretation requires additional verification.

Fig. 8 shows the dependence of D on the month of the given period in chronological order. It can be seen that the value of D exhibits a spread within the confidence interval. The presented results confirm the stability of the variations in D in different seismic periods.

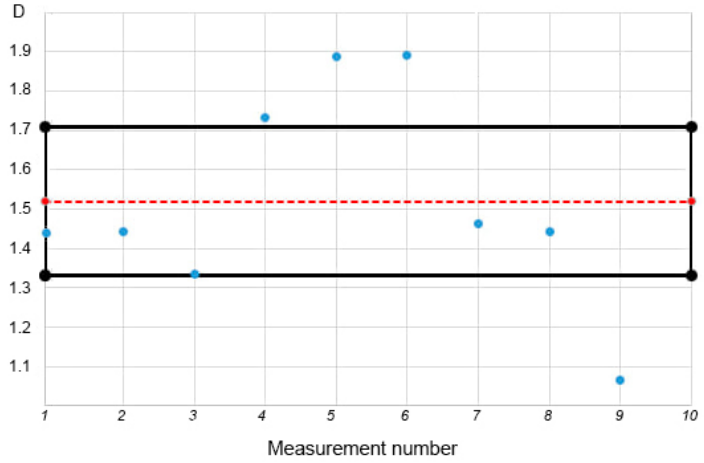

Fig. 8. Estimated confidence intervals for monthly mean values of parameter D obtained from Strainmeter III

Black horizontal lines mark the boundaries of the 95% confidence interval for the estimate of D. Red dashed line corresponds to the nominal (expected) value of $D = 1.51$

Conclusion

Analyzing the obtained results, we can draw the following conclusions.

1. Strainmeter III, located on a bedrock foundation, showed more pronounced changes in fractal parameters than strainmeters on sandy soil, since damping reduces sensitivity to small oscillations.

2. A decrease in singularity exponents $\Delta\alpha(q)$ and their spread during seismically active periods was observed for all strainmeters. This result may suggest a reorganization in the structure of the Earth's crust, however, the accuracy of determining the parameter $\Delta\alpha(q)$ also depends on the spread of the initial data, which was not analyzed in detail here.

3. All strainmeters showed similar changes in fractal characteristics in the periods from October 1, 2020 to March 31, 2021 and from January 15 to March 16, 2022, when the earthquakes occurred in Namie, Japan. These changes can serve as indicators of impending seismic events, but their qualitative interpretation requires further study.

4. The data from all strainmeters show abnormal behavior of fractal characteristics for the period from December 1, 2022 to February 15, 2023, suggesting the influence of an earthquake that occurred at the same time in Turkey or another seismic event. This period should be further analyzed to identify possible correlations and to clarify the nature of the detected anomalies.

Constant seismic activity does not subside in the area where the strainmeters are located, making it difficult to identify completely quiet periods, additionally affecting the strainmeter readings and subsequent interpretation of the results.

The conclusions presented in this paper indicate the potential predictive significance of such quantities as the fractal dimension D and the multifractal spectrum width $\Delta\alpha(q)$. However, these conclusions are preliminary and require additional confirmation.

REFERENCES

1. **Bak P., Tang Ch., Wiesenfeld K.,** Self-organized criticality, Phys. Rev. A. 38 (1) (1988) 364–374.

2. **Higuchi T.,** Relationship between the fractal dimension and the power law index for a time series: A numerical investigation, Physica D. 46 (2) (1990) 254–264.

3. **Kantelhard J. W., Zschiegner S. A., Koscielny-Bunde E., et al.,** Multifractal detrended fluctuation analysis of nonstationary time series, Physica A. 316 (1–4) (2002) 87–114.

4. **Dolgikh G. I., Privalov V. E.,** Lazernaya fizika. Fundamentalnye i prikladnye issledovaniya [Laser physics. Basic and applied research], Reya Publishing, Vladivostok, 2016 (in Russian).

5. **Lyubushin A. A.,** Analiz dannykh sistem geofizicheskogo i ehkologicheskogo monitoringa [Analysis of data from geophysical and environmental monitoring systems], Nauka Publishing, Moscow, 2007 (in Russian).

6. **Nasonov A. N., Tsvetkov I. V., Zhogin I. M., et al.,** Fraktaly v naukakh o Zemle [Fractals in the Earth's sciences], "Kovcheg" Publishing, Voronezh, 2018 (in Russian).

7. **Filatov D. M., Lyubushin A. A.,** Assessment of seismic hazard of the Japanese islands based on fractal analysis of GPS time series, Izv. Phys. Solid Earth. 53 (4) (2017) 545–555.

8. **Liehr L., Massopust P.,** On the mathematical validity of the Higuchi method, Phys. D. 402 (15 Jan) (2020) 132265.

9. **Mohamed H., Henares J., Peláez J., Damerdji Y.,** Fractal analysis of earthquake sequences in the Ibero-Maghrebian region, Pure Appl. Geophys. 176 (4) (2019) 1397–1416.

СПИСОК ЛИТЕРАТУРЫ

1. **Bak P., Tang Ch., Wiesenfeld K.** Self-organized criticality // Physical Review A. 1988. Vol. 38. No. 1. Pp. 364–374.

2. **Higuchi T.** Relationship between the fractal dimension and the power law index for a time series: A numerical investigation // Physica D: Nonlinear Phenomena. 1990. Vol. 46. No. 2. Pp. 254–264.

3. **Kantelhard J. W., Zschiegner S. A., Koscielny-Bunde E., Havlin S., Bunde A., Stanley H. E.** Multifractal detrended fluctuation analysis of nonstationary time series // Physica A: Statistical Mechanics and its Applications. 2002. Vol. 316. No. 1–4. Pp. 87–114.

4. **Долгих Г. И., Привалов В. Е.,** Лазерная физика. Фундаментальные и прикладные исследования. Владивосток: Изд. ООО «Рея», 2016. 352 с.

5. **Любушин А. А.** Анализ данных систем геофизического и экологического мониторинга. М.: Наука, 2007. 228 с.

6. **Насонов А. Н., Цветков И. В., Жогин И. М., Кульнев В. В., Репина Е. М., Кирносов С. Л., Звягинцева А. В., Базарский О. В.** Фракталы в науках о Земле. Воронеж: Типография ООО «Ковчег», 2018. 82 с.

7. **Филатов Д. М., Любушин А. А.** Оценка сейсмической опасности японских островов на основе фрактального анализа временных рядов GPS // Физика Земли, 2017. № 4. С. 55–66.

8. **Liehr L., Massopust P.** On the mathematical validity of the Higuchi method // Physica D: Nonlinear Phenomena. 2020. Vol. 402. 15 January. P. 132265.

9. **Mohamed H., Henares J., Peláez J., Damerdji Y.** Fractal analysis of earthquake sequences in the Ibero-Maghrebian region // Pure and Applied Geophysics. 2019. Vol. 176. No. 4. Pp. 1397–1416.

THE AUTHORS

LISOVITSKY Artem S.
V. I. Il'ichev Pacific Oceanological Institute
43 Baltiyskaya St., Vladivostok, 690041, Russia
lisovitckii.as@poi.dvo.ru ORCID: 0009-0006-5255-5894

CHUPIN Vladimir A.
V. I. Il'ichev Pacific Oceanological Institute
43 Baltiyskaya St., Vladivostok, 690041, Russia
chupin@poi.dvo.ru
ORCID: 0000-0001-5103-8138

MOSKOVCHENKO Larisa G.
Far Eastern Federal University
8 Suhanov St., Vladivostok, 690950, Russia
moskovchenko.lg@dvfu.ru
ORCID: 0000-0003-2621-0594

СВЕДЕНИЯ ОБ АВТОРАХ

ЛИСОВИЦКИЙ Артем Сергеевич – *аспирант лаборатории физики геосфер Тихоокеанского океанологического института имени В. И. Ильичёва Дальневосточного отделения РАН.*
690041, Россия, г. Владивосток, Балтийская ул., 43
lisovitckii.as@poi.dvo.ru
ORCID: 0009-0006-5255-5894

ЧУПИН Владимир Александрович – *доктор физико-математических наук, заведующий лабораторией физики геосфер Тихоокеанского океанологического института им. В. И. Ильичёва Дальневосточного отделения РАН.*
690041, Россия, г. Владивосток, Балтийская ул., 43
chupin@poi.dvo.ru
ORCID: 0000-0001-5103-8138

МОСКОВЧЕНКО Лариса Григорьевна – *кандидат физико- математических наук, доцент департамента теоретической физики и интеллектуальных технологий Дальневосточного федерального университета.*
690950, Россия, г. Владивосток, ул. Суханова, 8
moskovchenko.lg@dvfu.ru
ORCID: 0000-0003-2621-0594

Received 28.03.2025. Approved after reviewing 19.05.2025. Accepted 26.05.2025.
Статья поступила в редакцию 28.03.2025. Одобрена после рецензирования 19.05.2025. Принята 26.05.2025.